

Electronic Supplementary Information for

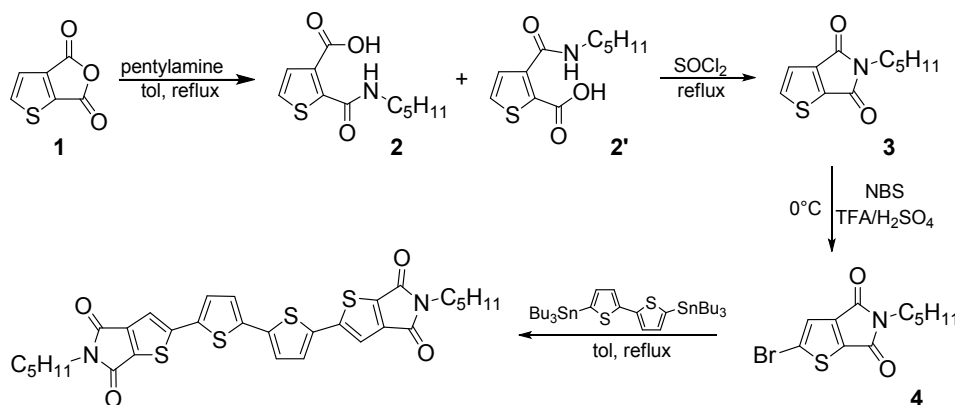
**Chemical design enables control of conformational polymorphism in
functional 2,3-thieno(bis)imide-ended materials**

Contents:

1. Synthesis of C5-NT4N.....	pg.2
2. Crystal Structure determination.....	pg.3
2.1 Single crystal structure of C3-NT4N form B.....	pg. 4
2.2 Structure determination of C4-NT4N form B.....	pg. 5
2.3 Single crystal structure of C5-NT4N form B.....	pg. 7
2.4 Single crystal structure of C6-NT4N form A.....	pg. 8
3. Photoluminescence of C4-NT4N powder form A and B.....	pg. 9
4. Differential scanning calorimetry (DSC).....	pg.10
5. Theoretical Calculations.....	pg.14
6. Thin-film/single crystal XRD comparison for C4-NT4N.....	pg.15
7. Thin deposits and thermal processing.....	pg.15
8. Thermal behavior of C3-NT4N.....	pg.15
9. References.....	pg. 16

1. Synthesis of C5-NT4N

General. TLC was carried out on Merk silica gel 60 F254 plates; detection by UV (254 nm, and 365 nm). Melting point was determined on a 'hot-stage' apparatus where the melting was observed with the aid of a microscope. All NMR spectra were recorded at room temperature using a Varian Mercury 400 spectrometer (^1H : 400 MHz; ^{13}C : 100.6 MHz). Chemical shifts are referenced to the residual solvent signal (CHCl_3 : δ ^1H = 7.26 ppm, δ ^{13}C = 77.16 ppm), respectively. Mass spectra were obtained with a Trace 1300 GC coupled to an ISQ mass spectrometer (Thermo Scientific) controlled by a computer running XCalibur software. According to the mass to be detected two different analytical approaches were employed, gas chromatography mass spectrometry (GC-MS) and direct exposure electron ionization mass spectrometry (DE-MS). UV-Vis spectra were recorded using a Perkin Elmer Lambda 20 spectrometer. Photoluminescence spectra in solution were obtained with a Perkin Elmer LS50B spectrofluorometer using an excitation wavelength corresponding to the maximum absorption lambda.



Scheme S1. Synthetic route to C5-NT4N.

3-(pentylcarbamoyl)thiophene-2-carboxylic acid and 2-(pentylcarbamoyl)thiophene-3-carboxylic acid (**2**)+(**2'**):

To a solution of **1** (600 mg, 3.9 mmol) in 60 ml of dry toluene, pentylamine (356 mg, 4.09 mmol) was added at room temperature, and the mixture was then refluxed for 48 h. After cooling to room temperature, the solvent was removed and the resulting crude was washed several times with pentane. 751 mg of a whitish solid were obtained. (Y = 80%).

^1H NMR (CDCl_3 , TMS/ppm) δ 7.74 (d, $^3J=4.8$ Hz, 1H), 7.54 (d, $^3J=5.2$ Hz, 1H), 7.40 (d, $^3J=5.6$ Hz, 1H), 7.38 (d, $^3J=5.6$ Hz, 1H), 7.20 (broad s, 2H), 3.47 (m, 4H), 1.66 (m, 4H), 1.36 (m, 8H), 0.91 (t, 6H).

5-pentyl-5H-thieno[2,3-c]pyrrole-4,6-dione (**3**):

A solution of **2+2'** (676 mg, 2.80 mmol) in 48 ml of SOCl_2 was refluxed under inert atmosphere for 4h. SOCl_2 was removed by distillation and the crude product was purified by flash chromatography on silica gel (Petr. Eth. : AcOEt = 9:1). Compound **3** was obtained as a yellow oil (558 mg, Y = 89%).

EI-MS m/z 223 (M^+). ^1H NMR (CDCl_3 , TMS/ppm) δ 7.74 (d, $^3J=4.8$ Hz, 1H), 7.30 (d, $^3J=4.8$ Hz, 1H), 3.59 (t, 2H), 1.65 (m, 2H), 1.33 (m, 4H), 0.89 (t, 3H). ^{13}C NMR (CDCl_3 , TMS/ppm) δ 164.0, 162.8, 144.7, 140.9, 137.2, 121.1, 38.5, 28.9, 28.5, 22.3, 13.9.

2-bromo-5-pentyl-5H-thieno[2,3-c]pyrrole-4,6-dione (**4**):

Compound **3** (617 mg, 2.77 mmol) was dissolved in a mixture of trifluoroacetic acid (7.8 ml) and H_2SO_4 (1.4 ml). NBS (492 mg, 2.77 mmol) was added at 0°C and the reaction mixture was stirred at room temperature overnight. The mixture was then diluted with 30 ml of water and extracted three times with dichloromethane. The organic layer was dried over Na_2SO_4 and concentrated under vacuum. The crude product was purified by flash chromatography on silica gel (Petr. Eth.: AcOEt: CH_2Cl_2 = 90:5:5), to afford compound **4** as a white solid (729 mg, Y=87%).

EI-MS m/z 302 (M^+), ^1H NMR (CDCl_3 , TMS/ppm) δ 7.30 (s, 1H), 3.57 (t, 2H), 1.63 (m, 2H), 1.32 (m, 4H), 0.89 (t, 3H). ^{13}C NMR (CDCl_3 , TMS/ppm) δ 163.0, 162.0, 143.9, 140.5, 125.4, 123.8, 38.7, 28.9, 28.4, 22.2, 13.9.

2,2'-(2,2'-bithiophene-5,5'-diyl)bis(5-pentyl-5H-thieno[3,2-c]pyrrole-4,6-dione) (**C5-NT4N**):

To a refluxing toluene solution (33.5 ml) of compound **4** (328 mg, 1.09 mmol) and in situ-prepared $\text{Pd}(\text{AsPh}_3)_4$ (10 mol%, 56 mg of Pd_2dba_3 and 133 mg of AsPh_3) under N_2 atmosphere, 5,5'-bis(tributylstannyl)-2,2'-bithiophene (367 mg, 0.493 mmol) in dry toluene (3.7 ml), was added dropwise. The solution was refluxed for 48 h then the solvent was removed under vacuum and the crude product

purified by flash chromatography on silica gel (CH₂Cl₂ : AcOEt = 95:5). The product was crystallized from hot toluene and washed several times with pentane and finally obtained as an orange powder (223 mg, Y = 74%).

M.p. 274 °C, EI-MS *m/z* 608 (M⁺), λ_{max} (CH₂Cl₂), 450 nm, λ_{em} (CH₂Cl₂), 570 nm; ¹H NMR (CDCl₃, TMS/ppm) δ 7.33 (s, 2H), 7.26 (d, ³J=3.6 Hz, 2H), 7.18 (d, ³J=4.0 Hz, 2H), 3.60 (t, 4H), 1.65 (m, 4H), 1.33 (m, 8H), 0.90 (t, 6H). ¹³C NMR (CDCl₃, TMS/ppm) δ 163.9, 162.7, 149.3, 145.3, 137.8, 137.6, 134.7, 126.8, 125.4, 116.7, 38.6, 28.9, 28.5, 22.3, 13.9. EI. Anal. Calcd for C₃₀H₂₈N₂O₄S₄ (608.09): C, 59.18; H, 4.64. Found: C, 59.11; H, 4.58.

2. Crystal Structure determination

Crystal data for **C3-NT4N form B**, **C5-NT4N form B**, **C6-NT4N form A** were collected on Oxford Diffraction Xcalibur S with Mo-Kα radiation, λ = 0.71073 Å, monochromator graphite. Crystal data and details of measurements are summarized in Table S1. SHELX97 [1] was used for structure solution and refinement based on F². CCDC 1033185-1033188 contains the supplementary crystallographic data for this paper. These data can be obtained free of charge via www.ccdc.cam.ac.uk/conts/retrieving.html (or from the Cambridge Crystallographic Data Centre, 12 Union Road, Cambridge CB2 1EZ, UK; fax: (+44)1223-336-033; or e-mail: deposit@ccdc.cam.ac.uk).

	C3-NT4N form B	C4-NT4N form B *	C5-NT4N form B	C6-NT4N form A
Formula	C ₂₆ H ₂₀ N ₂ O ₄ S ₄	C ₂₈ H ₂₄ N ₂ O ₄ S ₄	C ₃₀ H ₂₈ N ₂ O ₄ S ₄	C ₃₂ H ₃₂ N ₂ O ₄ S ₄
Formula weight	552.68	580.76	608.78	636.84
Crystal dimension (mm ³)	0.18 x 0.12 x 0.02	powder	0.34 x 0.04 x 0.02	0.29 x 0.04 x 0.01
Crystal system	Triclinic	Triclinic	Triclinic	Triclinic
Space group	P-1	P-1	P-1	P-1
a (Å)	5.265(1)	5.127(3)	5.289(2)	4.6152(7)
b (Å)	5.473(5)	5.526(2)	5.474(2)	11.558(1)
c (Å)	22.49(3)	25.038(2)	25.81(2)	14.422(2)
α (°)	87.9(1)	84.04(3)	85.15(5)	80.38(1)
β (°)	87.40(6)	89.75(4)	84.36(4)	88.11(1)
γ (°)	87.05(6)	86.19(7)	87.27(3)	86.45(1)
Volume (Å ³)	646.1(11)	704.1(1)	740.1(6)	756.8(2)
Z	1	1	1	1
δ (g/mL)	1.420	1.370	1.370	1.397
μ (mm ⁻¹)	0.404	-	0.359	0.355
λ (Å)	0.71073	1.5418	0.71073	0.71073
Temp K	293(2)	293(2)	293(2)	293(2)
Reflections (measured/independent)	5814/ 2522	-	1671/1406	5206/3000
R _{int}	0.0477	-	0.0605	0.0732
R	0.0693	0.08033 (Rp)	0.1390	0.0890
wR (all data)	0.1322	0.10699 (Rwp)	0.4279	0.2032
Residual electron density (e.Å ⁻³)	0.323	-	0.287	0.419

* Structure determination from X-ray powder diffraction data.

2.1 Single crystal structure of C3-NT4N form B

A small crystal suitable for X-ray single crystal diffraction was obtained in the DSC pan by cooling melted C3-NT4N. Non-hydrogen atoms were refined anisotropically. Hydrogen atoms were added in calculated positions. The molecule C3-NT4N is located on the inversion center. The core of the molecule is planar as observed in several thiophene compounds and the torsion angles between the thiophene rings in *syn* conformation is 1.13° .

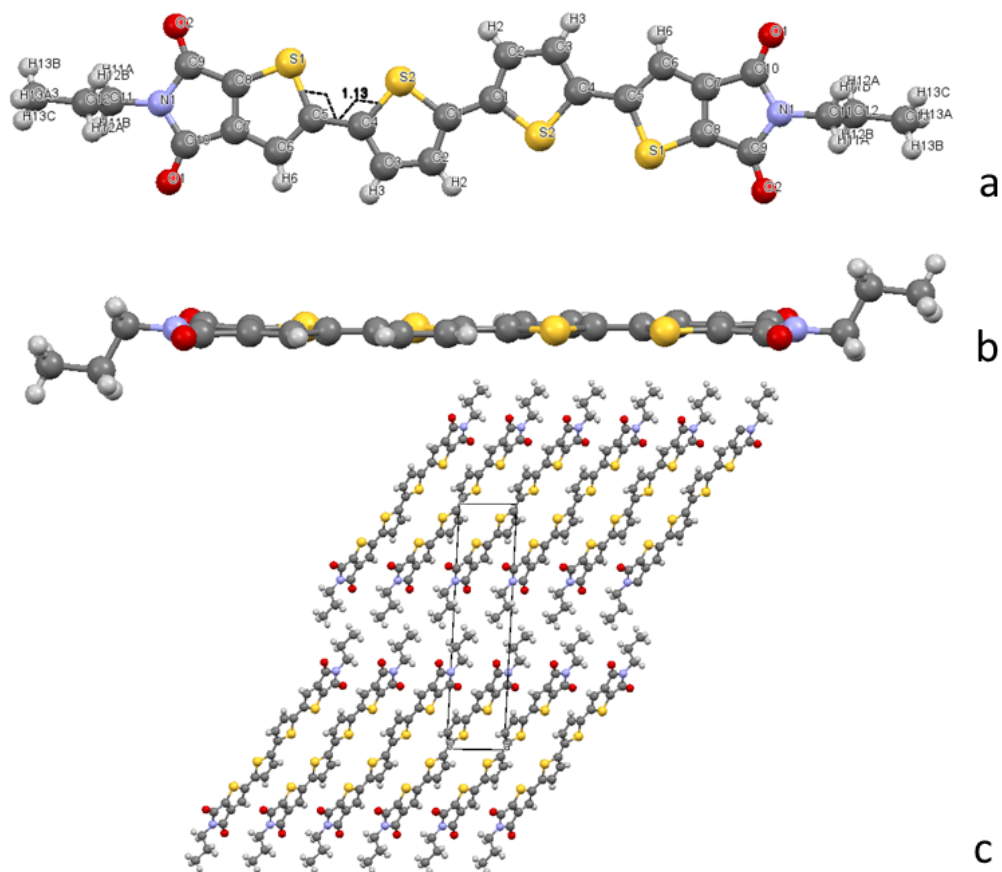


Figure S1. a) Structure of C3-NT4N with labels and torsion angle between the S atoms in *syn* conformation (1.13°). The S atoms in *anti* are related by the inversion point. b) Side view of the molecule C3-NT4N. c) packing view along the b axis

2.2 Structure determination of C4-NT4N form B

C4-NT4N phase B has been solved from high resolution x-ray powder diffraction data collected on an Philips PW3040/60 X'Pert Pro diffractometer with Cu-K α (K α 1: 1.540598 Å, K α 2: 1.5444260 Å) radiation at room temperature. A single graphite X'Celerator monochromator (diffraction angle, θ_m : 13.265313°) has been used. The tube voltage and the tube current were 40 kV and 40 MA respectively. The 2 θ scan range was from 3 to 60° with a step size of 0.02° and counting time of 3 sec per step. The powder diffraction pattern was indexed using X-Cell [2] implemented in Reflex Plus module in MS 6.1 program (Accelrys Co., Ltd., USA). The space group has been determined from the peak intensities obtained by Pawley refinement [3].

The crystal structure solution has been achieved through a self-consistent iterative four-step process. In the first step, a preliminary guess of the atomic coordinates in the asymmetric unit cell was obtained by the use of a Monte Carlo/parallel tempering algorithm as implemented in Powder Solve code [4].

The solution was then improved through the Rietveld refinement of various parameters (e.g. profile, background, lattice constants, zero point shift, atomic coordinates). Preferred orientation correction accounting for deviation from random crystallite orientation has been considered according to March-Dollase equation [5].

In the third step, the crystal structure with the lowest figure of merit, R_{wp} , that means the best similarity between the experimental powder data and the simulated powder patterns, was optimized by periodic density functional theory (DFT) calculations with the hybrid B3LYP functional [6-7]. The Kohn–Sham orbitals were expanded in Gaussian type orbitals, as implemented in CRYSTAL09 package[8-9]. The basis sets adopted were 6-31(d1) for oxygen, [10] nitrogen [11] and carbon, [12] 31(p1) for hydrogen [11] and 8-6311(d1) for sulphur [13]. The condition for SCF convergence was set to 10⁻⁶ hartree, the reciprocal space was sampled by a 2 x 2 x 2 k-point mesh corresponding to 8 k-points of the irreducible Brillouin zone and the atomic positions were fully relaxed until the largest component of the ionic forces was less than 4.5E-4 a.u. [14]. Long-range dispersion interactions, of primary importance in molecular crystals, are accounted by a post-DFT dispersive contribution, suggested by Grimme, [15] to the computed ab initio total energy and gradients. Such correction has been recently implemented in the CRYSTAL code and has been successfully validated in particular in combination with the B3LYP functional. [16-17] Van der Waals radii and dispersion coefficients C6 were taken from Table 1 of reference [15]. During the DFT structural optimization lattice constants were kept fixed. In the last step, the structural solution, corresponding to an electronic energy minimum, was subjected to a Rietveld refinement with both lattice constants and atomic coordinates frozen. The resulting solution became the initial guess of a new cycle until no significant variations between subsequent cycle solutions was observed. The final Rietveld refinement was performed with the software TOPAS 4. A shifted Chebyshev function with 10 parameters and a Pseudo-Voigt function (TCHZ type) were used to fit background and peak shape, respectively. C4-NT4N molecule was described as rigid body and only the torsion angle S1-C2-C5-S10 and the torsion angles of the alkyl chain were refined. A spherical harmonics model was used to describe preferred orientation. Refinement converged with $\chi^2 = 2.863$, $R_{wp} = 10.699\%$, $R_b = 1.61\%$ (see difference plot fig S2).

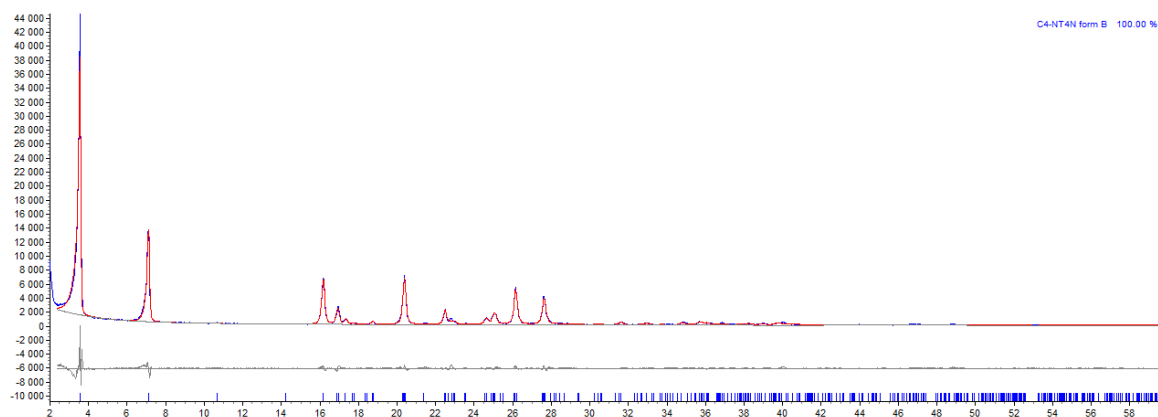


Figure S2. Experimental (Blue line), calculated (red line) and difference (grey line) patterns for C4-NT4N form B. The molecule C4-NT4N is located on the inversion center. The core of the molecule is planar as observed in several thiophene compounds and the torsion angles between the thiophene rings in *syn* conformation is -7.07° (see figure S3).

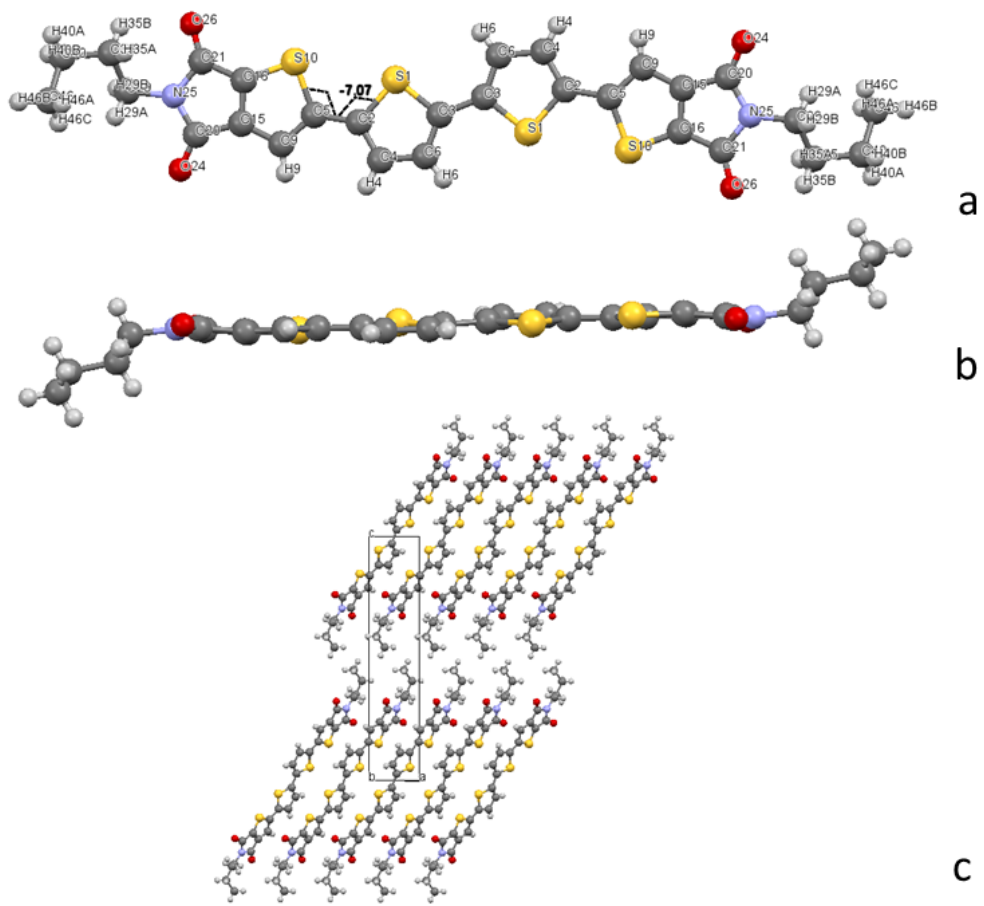


Figure S3. a) Structure of C4-NT4N with labels and torsion angle between the S atoms in *syn* conformation (-7.07°). The S atoms in *anti* are related by the inversion point. b) Side view of the molecule C4-NT4N. c) packing view along the b axis

2.3. Single crystal structure of C5-NT4N form B

Very small crystals suitable for X-ray single crystal diffraction were obtained by vapour diffusion of ether in a CH_2Cl_2 solution of C5-NT4N. The small dimension of the crystals did not allow a complete data collection. Only sulphur atoms were refined anisotropically. Hydrogen atoms were added in calculated positions. The molecule C5-NT4N is located on the inversion center. The core of the molecule is planar as observed in several thiophene compounds and the torsion angle between the thiophene rings in *syn* conformation is 3.81° (figure S4).

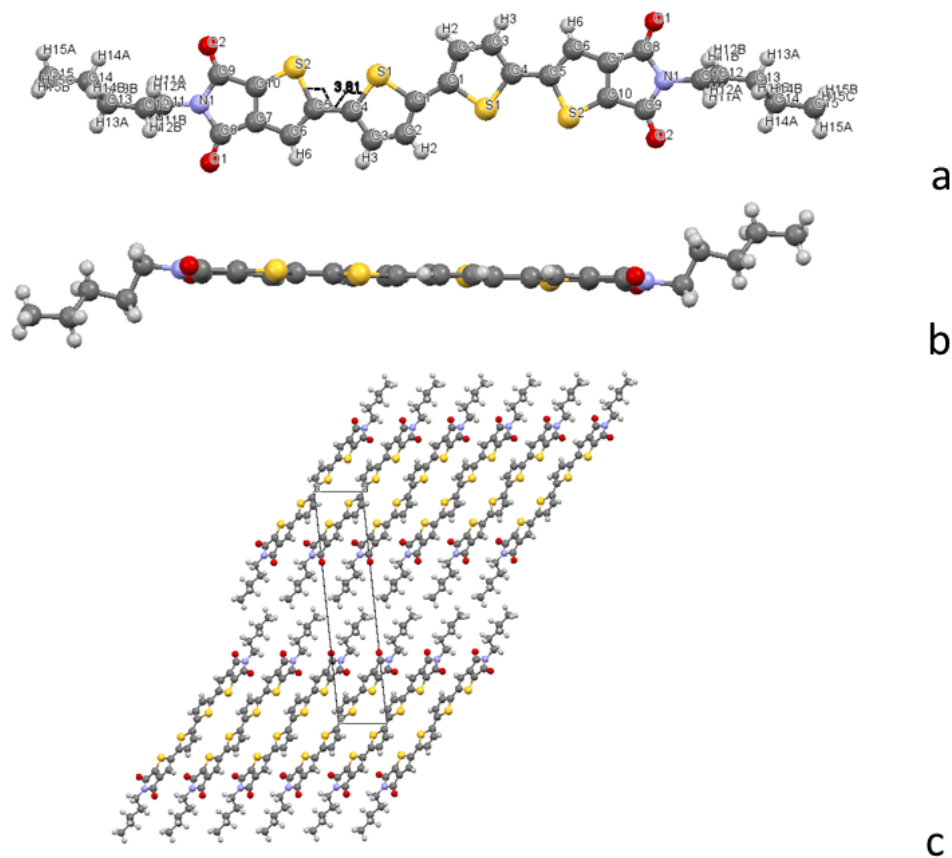


Figure S4. a) Structure of C5-NT4N with labels and torsion angle between the S atoms in *syn* conformation (3.81°). The S atoms in *anti* are related by the inversion point. b) Side view of the molecule C5-NT4N. c) packing view along the b axis

2.4 Single crystal structure of C6-NT4N form A

A small crystal suitable for X-ray single crystal diffraction was obtained by recrystallization of C6-NT4N in toluene. Non-hydrogen atoms were refined anisotropically. Hydrogen atoms were added in calculated positions. The molecule C6-NT4N is located on the inversion center. The core of the molecule is planar as observed in several thiophene compounds. (see figure S5)

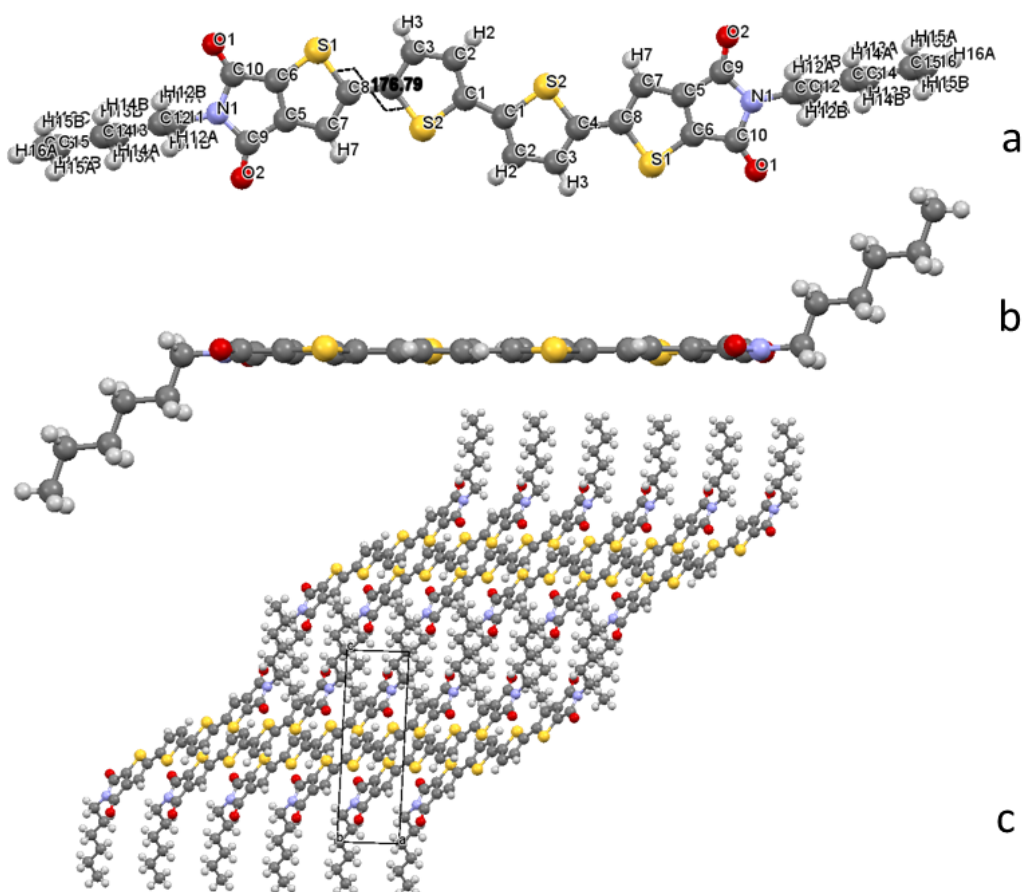


Figure S5. a) Structure of C6-NT4N with labels and torsion angle between the S atoms in *anti* conformation (176.79°) not related by the inversion point. b) Side view of the molecule C6-NT4N. c) packing view along the b axis.

3. Photoluminescence of C4-NT4N powder form A and B

PL emission was collected with a calibrated optical multichannel analyzer (PMA-11, Hamamatsu). Steady-state photoluminescence (PL) was excited using a CW He-Cd laser at 325 nm and collected in transmission conditions (no colour filter was necessary for truncating laser excitation).

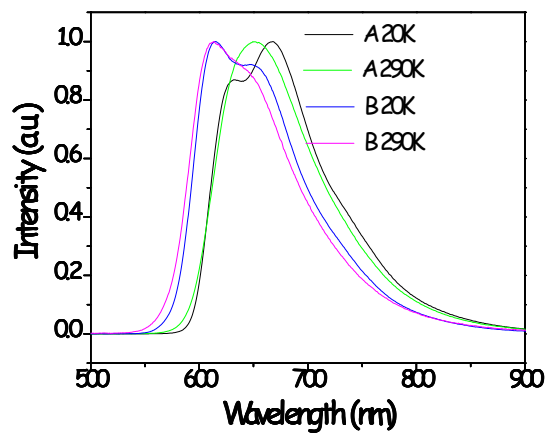


Figure S6. Emission of powder of C4-NT4N forms A and B at different temperature.

4. Differential scanning calorimetry (DSC)

Calorimetric measurements were performed using a Perkin Elmer Pyris Diamond DSC equipped with a model ULSP intracooler. Temperature and enthalpy calibration were performed using high-purity standards (n-decane and indium). Samples (3-5 mg) were placed in sealed aluminum pans. Heating and cooling were carried out at $5^{\circ}\text{C min}^{-1}$ for all samples.

The **C3-NT4N** crystallizes at room temperature as phase B' already reported in the literature [18] (refcode in CCDC: MODNUQ). The DSC curve of sample C3-NT4N shows an endothermic peak at 270°C which corresponds to the solid state transition $B' \rightarrow B$. The crystal structure of C3-NT4N form B is reported in this paper. The C3-NT4N converts to liquid crystal at 287°C and melts at 296°C (see figure S7a). The cooling thermogram presents the conversion liquid-liquid crystal at 293°C followed by the solidification at 277°C to form B (see figure S7b).

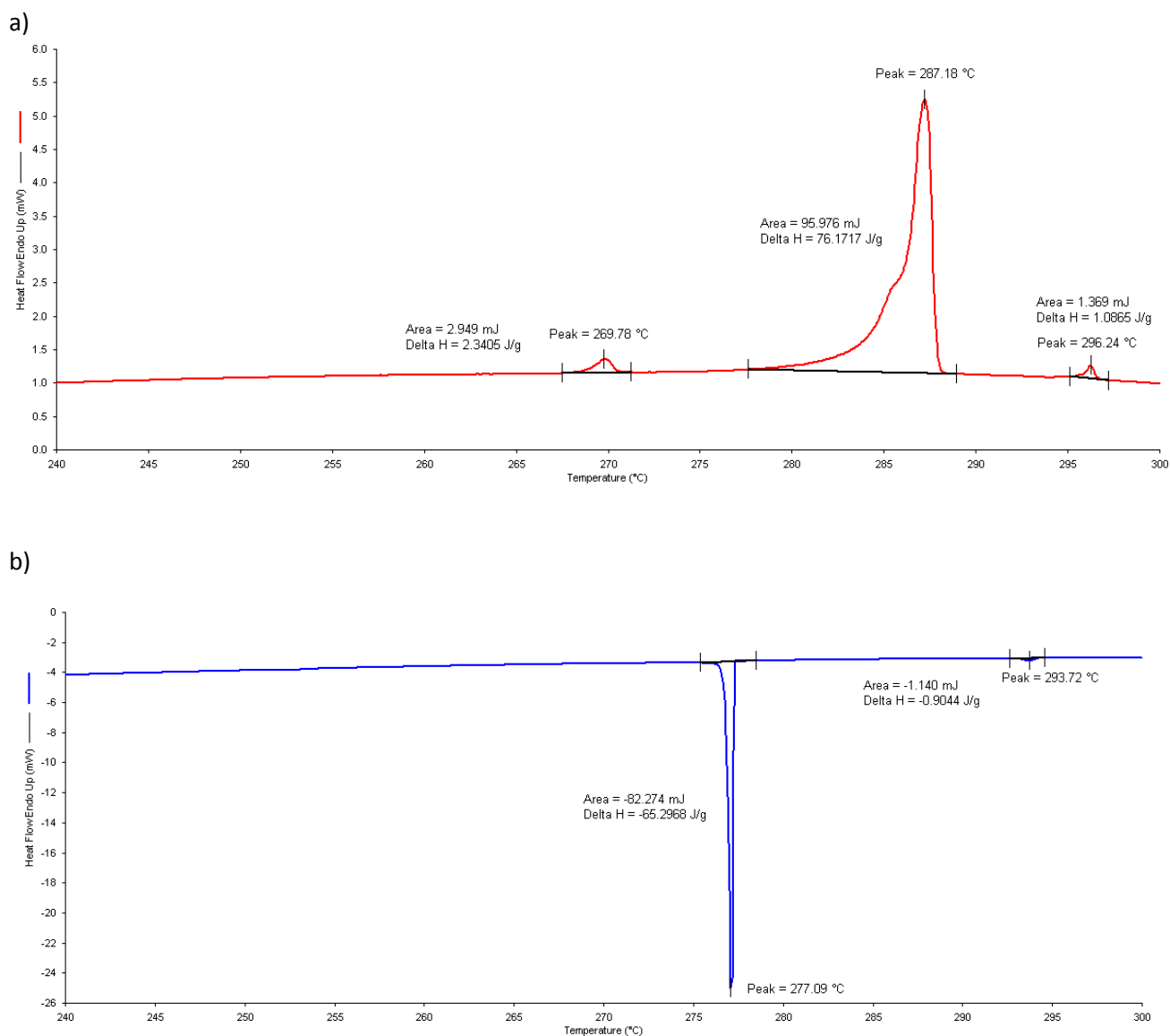
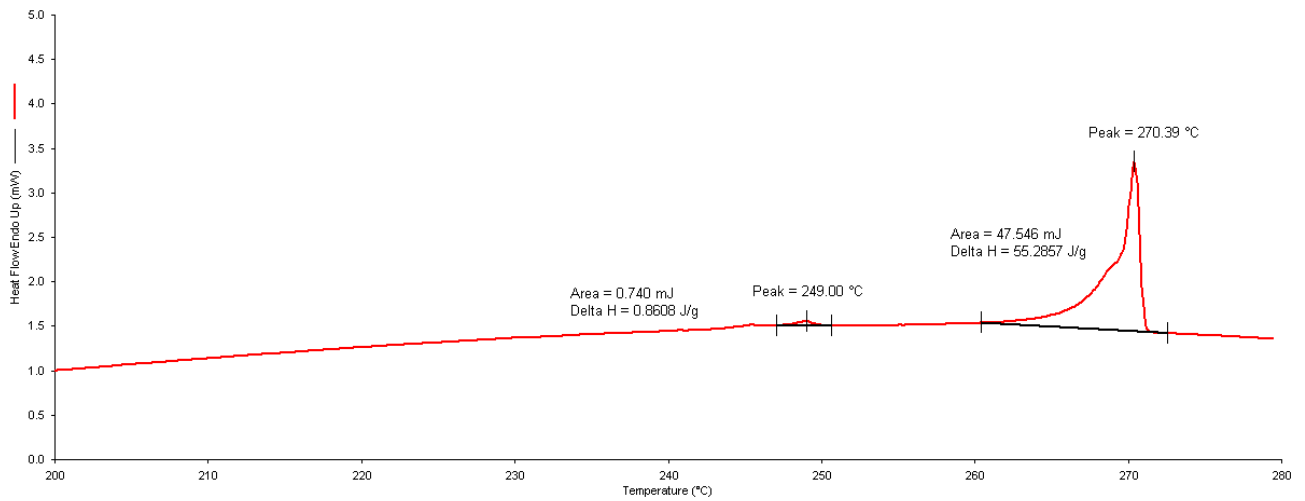


Figure S7. DSC form B C3-NT4N; heating a), cooling b)

The **C5-NT4N** crystallizes at room temperature as phase B. The DSC curve shows a endothermic peaks at 240°C . Although it was not possible to better characterize the new phase, the energy involved in the solid –solid transition can exclude a conformational change. The C5-NT4N converts to liquid crystal at 270° (see figure S8 a). The cooling thermogram presents the conversion liquid- liquid crystal at 293°C followed by the solidification at 277°C to form B (see figure S8b).

a)



b)

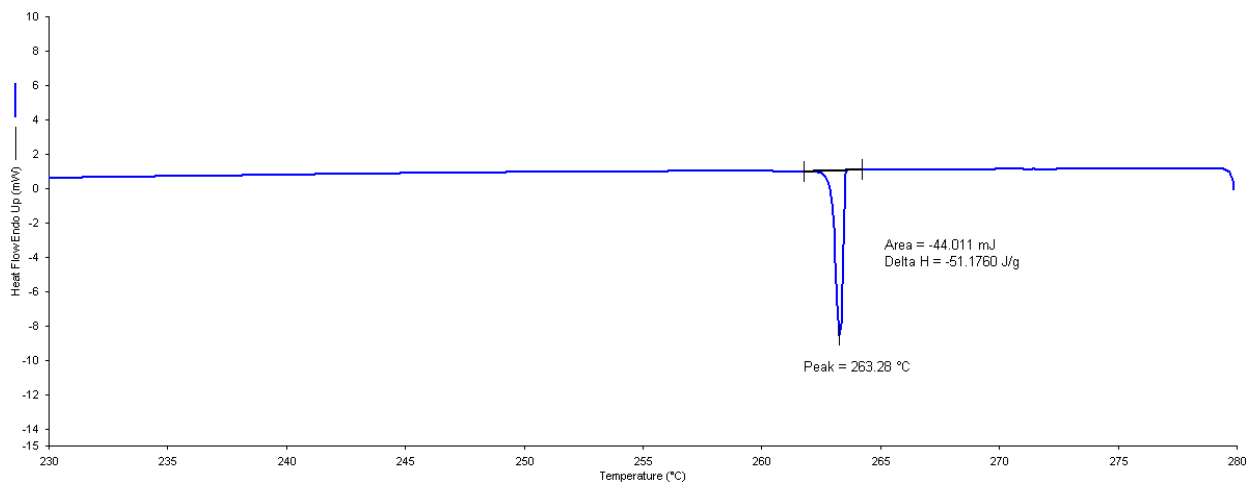
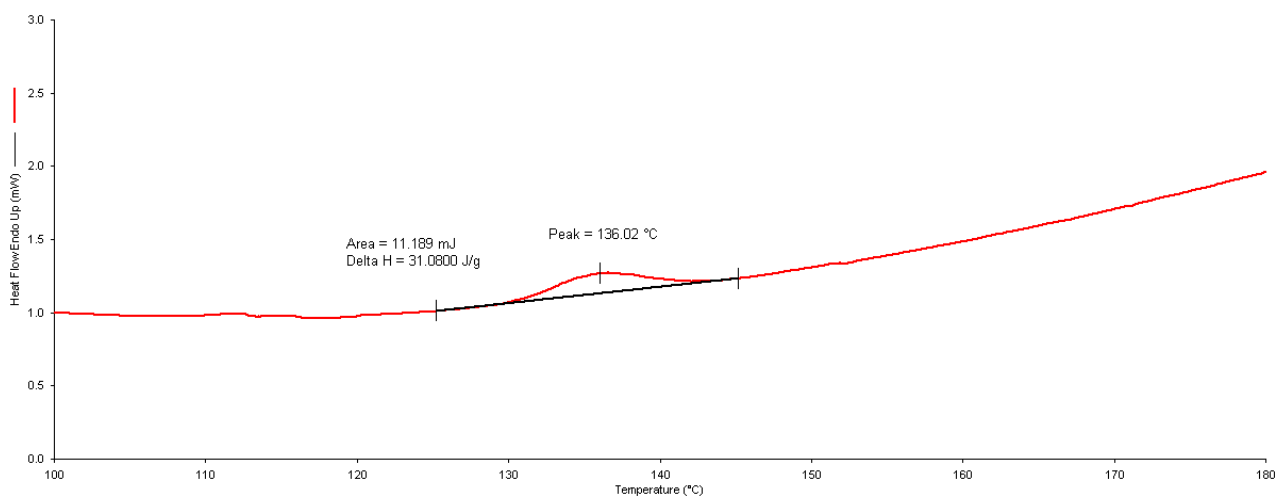


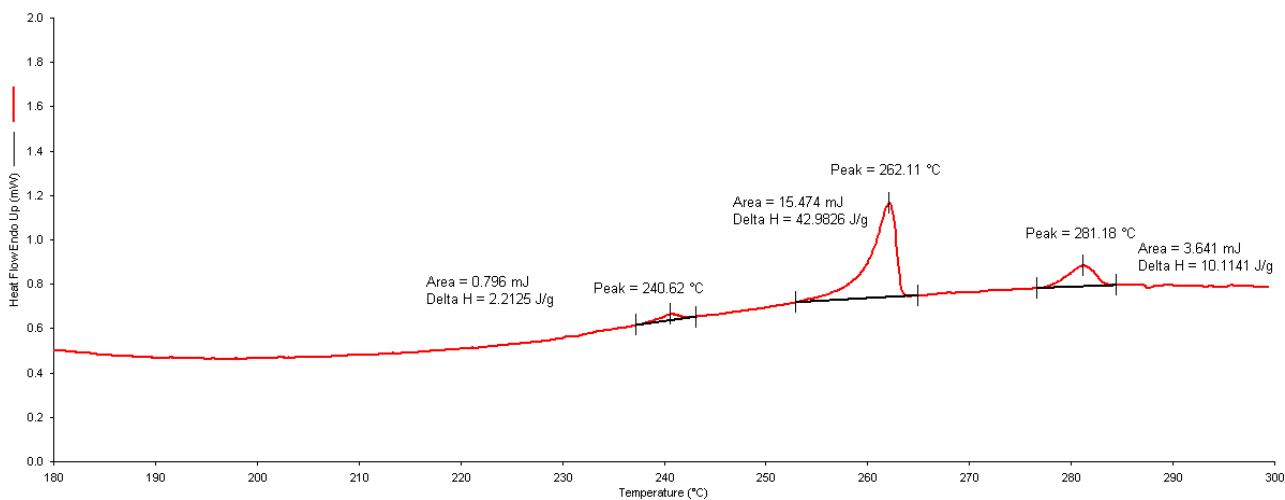
Figure S8. DSC form B C5-NT4N; heating a), cooling b)

The DSC curve of single crystals of **C6-NT4N** phase A presents an endothermic solid- solid transition at 136°C which corresponds to the conversion of phase A to phase B. Interestingly, phase B undergo to a further transition at 240°C followed by the solid to liquid crystal transition at 262°C. C6-NT4N melts at 282°C (see figure S9b). The cooling trace shows the liquid to liquid crystal transition followed by the solidification at 255°C (see figure S9c). The heating trace of C6-NT4N form B does not show events until 240°C (see figure S10a-b). At 242°C it is present the solid-solid transition as observed in sample C6-NT4N form A. The energy involved excludes the possibility of a conformational polymorph (see figure S10b). The new phase is stable only at high temperature as suggested by the exothermic peak at 236°C in the cooling trace (see figure S10c).

a)



b)



c)

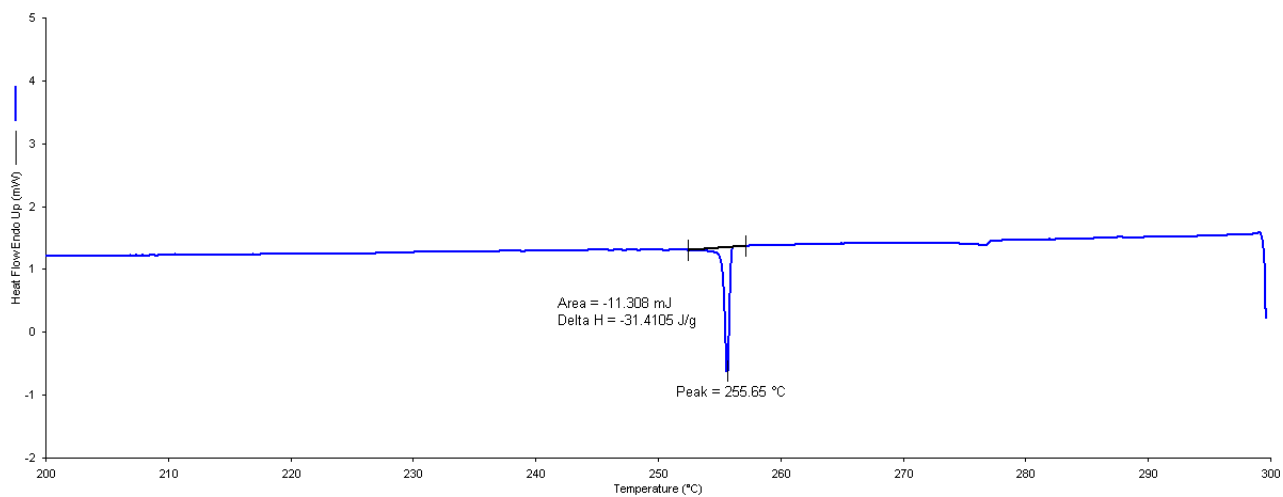
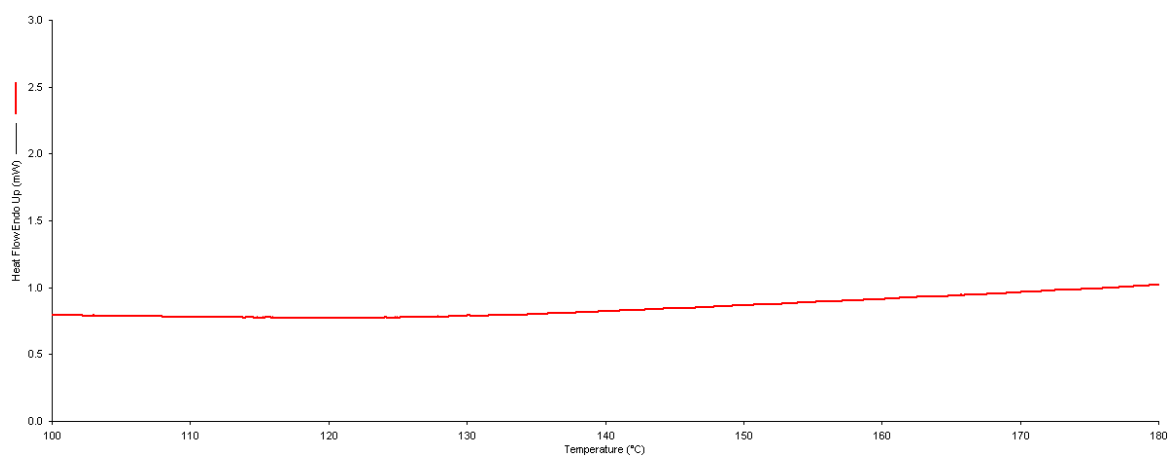
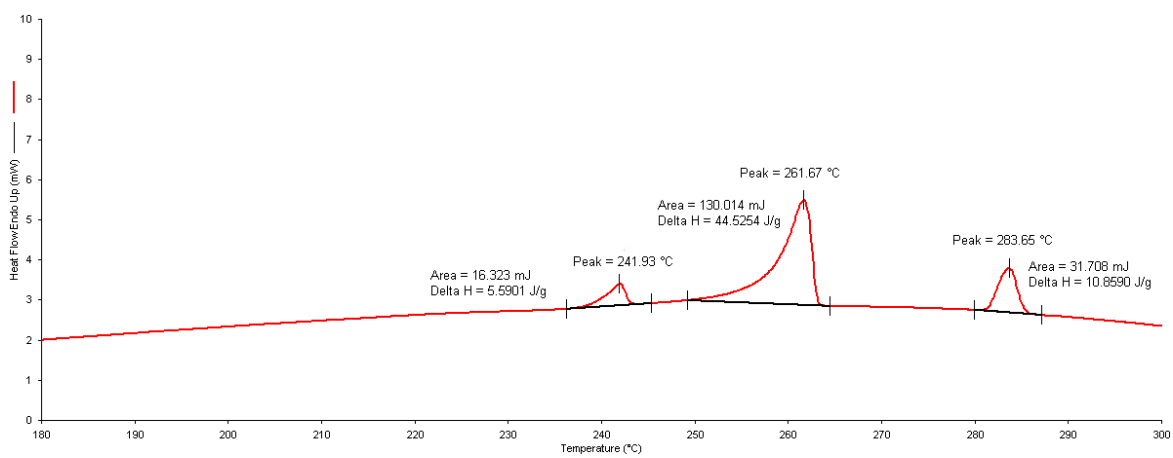


Figure S9. DSC Form A C6-NT4N; heating a) and b); cooling c).

a)



b)



c)

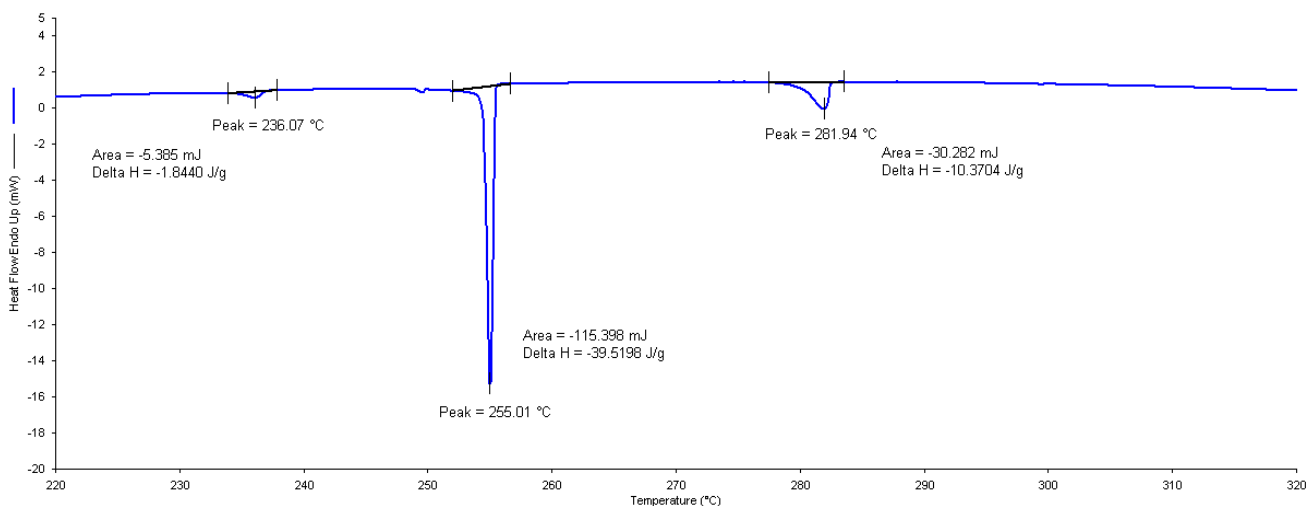


Figure S10. DSC Form B C6-NT4N; heating a) and b); cooling c).

5. Theoretical Calculations

Torsional energy barriers of C4-NT4N have been investigated through the hybrid exchange-correlation B3LYP functional [6-7] as implemented in the CRYSTAL09 package [8-9].

The all-electron Gaussian-type basis sets adopted were 6-31(d1) for oxygen [10], nitrogen [11] and carbon [12], 31(p1) for hydrogen [11] and 8-6311(d1) for sulphur [13]. During geometry optimizations, no symmetry restriction was imposed except for the torsional angles. In contrast, the absolute energy minimum was obtained by a complete geometry optimization. The SCF convergence was set to 10^{-7} , the threshold for the maximum and the root-mean-square (RMS) forces and the maximum and the RMS atomic displacements on all the atoms have been set to 0.000450 and 0.000300 a.u. and 0.001800 and 0.001200 a.u., respectively.

Long-range dispersion interactions were accounted by a post-DFT dispersive contribution, suggested by Grimme [15], to the computed ab initio total energy and gradients.

All energy values are scaled with respect to the absolute energy minimum, found at $\Phi_1 = \Phi_2 = 2.1^\circ$ and corresponding to the *anti-anti-anti* conformation.

6. Thin-film/single crystal XRD comparison for C4-NT4N

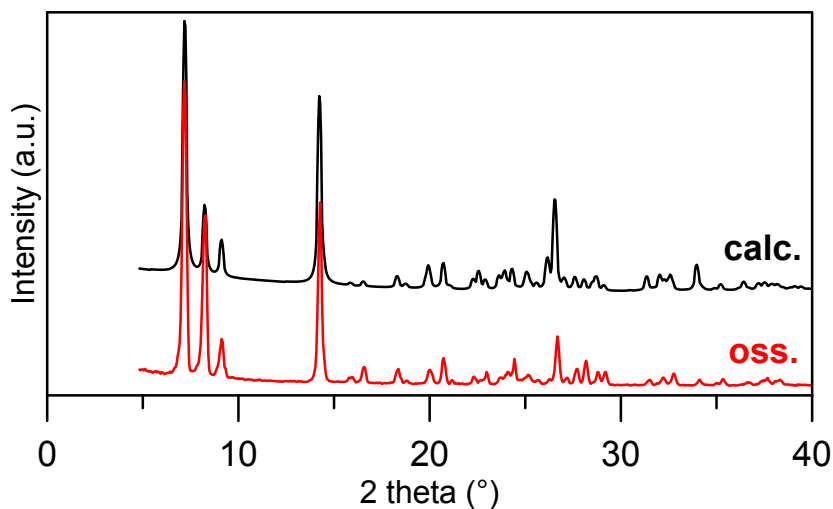


Figure S11. The XRD pattern calculated from single crystal data of A phase for C4-NT4N (black, [1] PowderCell program V3.2) is compared with the pattern of the solution casting sample (red). A slight parameter of preferential orientation parallel to plane 1 0 6 was taken into account in the calculation.

7. Thin deposits and thermal processing

Thin deposits. Thin deposits of all compounds were prepared by drop casting a toluene solution (20 $\mu\text{l}/\text{cm}^2$, 1 g/L) (Spectroscopy quality grade) on Si/SiO₂ wafers (10x10 mm² piece of silicon covered by 200 nm of thermal oxides, pre-cleaned by: sonication for 2 min in electronic-grade water (milli-pure quality), acetone then 2-propanol). The solvent was slowly evaporated at room temperature in a solvent-saturated atmosphere.

Thermal annealing. The thermal annealing were performed under the optical microscope using a heating stage Linkham TMHS600 connected to a TP94 controller, with a control of 0.1 °C .

8. Thermal behavior of C3-NT4N

Laser Scanning Confocal Fluorescence imaging was performed on an inverted Nikon A1 laser scanning confocal microscope equipped with a CW Argon ion laser (excitation at 488 nm, Melles Griot). Confocal fluorescence imaging was carried out on the samples at RT. The 521 x 512 or 1024 x 1024 pixel images were collected using a Nikon PLAN APO VC 60 oil immersion objective with NA 1.40. With this imaging configuration, pixel side dimension ranged from 100 to 250 nm. Hexagonal pinhole dimension was set to 0.8 au corresponding to 25 μm and optical thickness of 330 nm. In the scan head dichroic mirrors reflecting 488, 541 and 640 nm were used. Fluorescence intensity images were collected for several spectral windows using bandpass filters centered at 525 nm (50), 595 (50) and 700 nm (75). Spectral imaging has been performed using the Nikon A1 spectral detector consisting of a multi-anode photomultiplier with an array of 32 anodes. A wavelength range of 6 or 10 nm per anode has been applied.

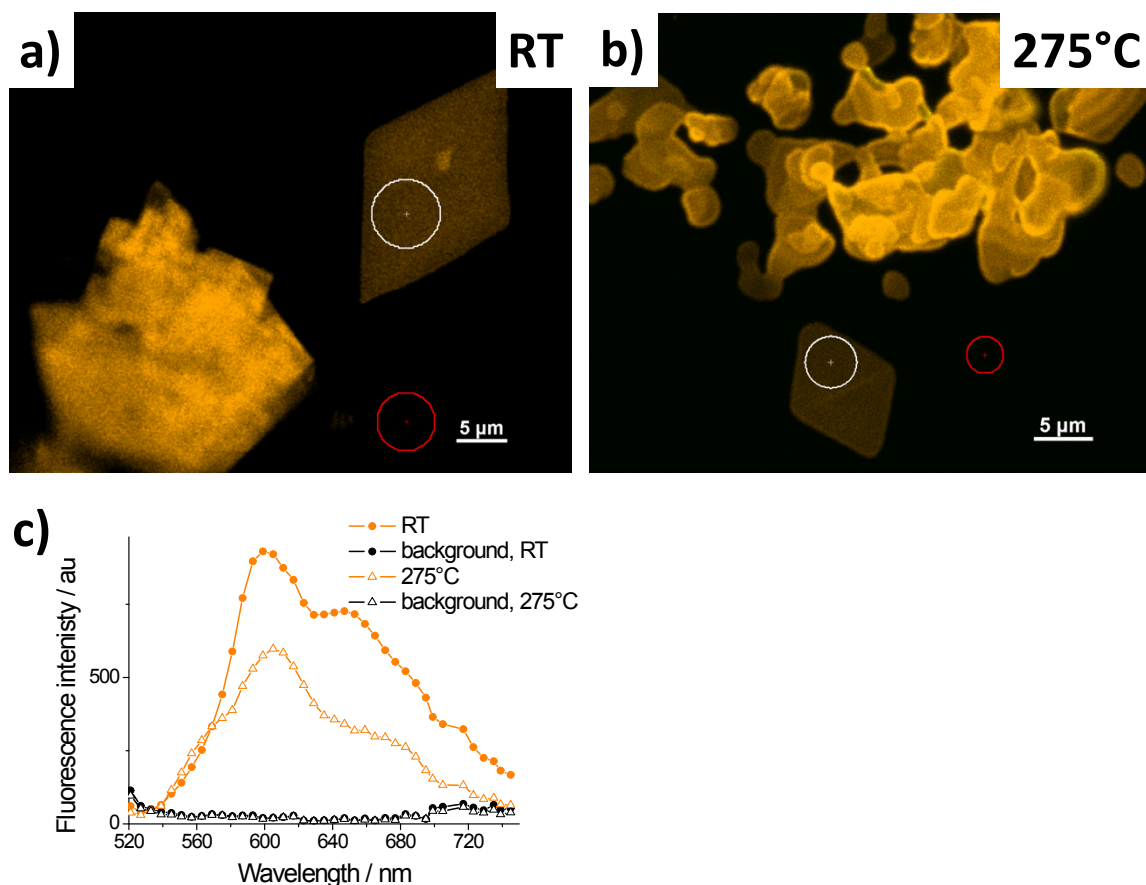


Figure S12. Confocal fluorescence images of thin deposits of sample C3-NT4N, kept at room temperature (a) and heated at 275°C (b). (c) The confocal fluorescence spectra of the regions indicated by the white circles and of the background (red circle).

9. References

- [1] G. Sheldrick, *Acta Crystallogr. Sect. A* 2008, 64, 112-122.
- [2] M. Nuemann, *J. Appl. Cryst.*, vol. 36, pp. 356-365, 2003.
- [3] A. J. Markvardsen, W. I. F. David, J. C. Johnson e K. Shankland, *Acta Cryst.*, vol. A57, pp. 47-54, 2000.
- [4] G. E. Engel, S. Wilke, O. König, K. D. M. Harris e F. J. J. Leusen, *J. Appl. Cryst.*, vol. 32, pp. 1169-1179, 1999.
- [5] W. A. Dollase, *J. Appl. Cryst.*, vol. 19, pp. 267-272, 1986.
- [6] A. D. Becke, *J. Chem. Phys.*, vol. 98, pp. 5648-5652, 1993.
- [7] C. Lee, W. Yang e R. G. Parr, *Phys. Rev. B*, vol. 37, pp. 785-789, 1988.
- [8] R. Dovesi, R. Orlando, B. Civalleri, C. Roetti, V. R. Saunders e C. M. Zicovich-Wilson, *Z. Kristallogr.*, vol. 2005, pp. 571-573, 2005.
- [9] R. Dovesi, V. R. Saunders, C. Roetti, R. Orlando, C. M. Zicovich-Wilson, F. Pascale, B. Civalleri, K. Doll, N. M. Harrison, I. J. Bush, P. D'Arco e M. Llunell, *CRYSTAL09 (CRYSTAL09 User's Manual)*, Torino: University of Torino, 2009.
- [10] M. Corno, C. Busco, B. Civalleri e P. Ugliengo, *Phys. Chem. Chem. Phys.*, vol. 8, pp. 2464-2472, 2006.
- [11] C. Gatti, V. R. Saunders e C. Roetti, *J. Chem. Phys.*, vol. 101, pp. 10686-10696, 1994.
- [12] M. A. Spackman e A. S. Mitchell, *Phys. Chem. Chem. Phys.*, vol. 3, pp. 1518-1523, 2001.

- [13] V. Maslyuk , C. Tegenkamp, H. Pfnur e T. Bredow, *ChemPhysChem*, vol. 7, pp. 1055-1061, 2006.
- [14] C. M. Zicovich-Wilson, F. Pascale, C. Roetti, V. R. Saunders, R. Orlando e R. Dovesi, *J. Comput. Chem.* , vol. 25, pp. 1873-1881, 2004.
- [15] S. Grimme, *J. Comput. Chem.*, vol. 27, pp. 1787-1799, 2006.
- [16] B. Civalleri, C. M. Zicovich-Wilson, L. Valenzano e P. Ugliengo, *Cryst. Eng. Comm.*, vol. 10, pp. 405-410, 2008.
- [17] P. Ugliengo, C. M. Zicovich-Wilson, S. Tosoni e B. Civalleri, *J. Mater. Chem.*, vol. 19, p. 2564, 2009.
- [18] M. Melucci, M. Durso, C. Bettini, M. Gazzano, L. Maini, S. Toffanin, S. Cavallini, M. Cavallini, D. Gentili, V. Biondo, G. Generali, F. Gallino, R. Capelli, M. Muccini, *J. Mater. Chem. C* **2014**, 2, 3448–3456.